EMP Theoretical Notes

Note 125

HAPS - A TWO-DIMENSIONAL HIGH ALTITUDE EMP ENVIRONMENT CODE

by

W. A. Radasky
Air Force Weapons Laboratory

and

R. L. Knight*
The Dikewood Corporation

Supported by
Defense Nuclear Agency
Subtask EA091

November 1971

* Presently at Science Applications, Inc.
335 Jefferson S. E., Albuquerque, New Mexico

HAPS - A TWO-DIMENSIONAL

HIGH ALTITUDE EMP ENVIRONMENT CODE

ABSTRACT

This report discusses the mathematical formulation of the field calculations and boundary conditions used in HAPS, the AFWL high-altitude EMP environment code. The finite difference scheme employed in the solution of these equations is also described. A final section exhibits some results of comparisons that have been made between HAPS and other environmental codes.

TABLE OF CONTENTS

Section		Page
	ABSTRACT	ii
I.	INTRODUCTION	1
II.	SOLUTION OF THE FIELD EQUATIONS	5
	1. Transverse Electric Fields	5
	2. Transverse Magnetic Fields	11
III.	BOUNDARY CONDITIONS	14
IV.	COMPARISON OF HAPS WITH OTHER EMP CODES	22
	REFERENCES	32

SECTION I. INTRODUCTION

This report describes a two-dimensional finite difference code, HAPS, that has been developed to calculate the electromagnetic pulse (EMP) generated by the high altitude detonation of a nuclear weapon at latitudes in which the earth's magnetic field is nearly vertical. The source presently used for the determination of these fields is a distribution of current in the atmosphere arising from Compton collisions of the weapon produced γ-rays with electrons in the air. It is anticipated that x-ray sources will be incorporated later. The turning of these Compton electrons by the earth's magnetic field is accounted for in an approximate way.

A previous high altitude code, HEMP, developed at AFWL by Capt. John Erkkila (1967) employs the high-frequency approximation of Karzas (1964) to reduce the intrinsically three-dimensional field calculation to one involving a single coordinate along the line of sight from the weapon to the observer. The original motivation for doing the present problem was to obtain a more exact solution from which a determination of the accuracy of this high-frequency approximation for later times of calculation could be made. Favorable comparisons of the two codes is given in Section IV along with comparisons of HAPS and B, the AFWL medium altitude code.

It is well known that an oscillating spherically symmetric current distribution will not radiate electromagnetic energy. For the high altitude problem this symmetry is destroyed by an asymmetry of the weapon, by

the density gradient of the atmosphere, by the influence of the earth's magnetic field on the sources, and at greater distances, by reflections from the surface of the earth. In general, these effects will jointly deprive the problem of all symmetry. The resulting calculation then involves six field components each of which is a function of three spatial dimensions and time.

To reduce the problem to a more manageable one, its scope has been limited in HAPS by the assumption of azimuthal symmetry, which implies the limitation on the orientation of the earth's magnetic field mentioned above, and in addition requires symmetry in the weapon's output. Although the number of field components to be calculated remains the same, the differential equations are simplified and the number of required spatial variables is reduced to two. This places much less stringent storage and calculation time requirements on the computer.

It has proven most realistic in the past to use weapon-centered coordinate systems in EMP environment calculations because the solution of an EMP problem requires a boundary condition at the outer edge of the mesh. In addition an inner boundary is often employed to prevent numerical instabilities. These boundary conditions are most conveniently specified along lines of constant coordinate. A problem occurs, however, when attempting to simulate the surface of the earth for reflection purposes with, for example, a spherical bomb-centered coordinate system. Because of these considerations, HAPS was written in prolate spheroidal coordinates. By approximating the earth's surface with one of the hyperbolas of the prolate

spheroidal coordinate system, the problem of reflection can be handled adequately. As for the inner boundary condition, a hyperbola above the source region has proven successful in actual calculations. Interestingly, lines of constant radius from the weapon can also be mapped over the prolate spheroidal grid with little difficulty.

The azimuthal symmetry reduces Maxwell's equations to two sets of uncoupled differential equations that determine the transverse electric fields (E_ϕ, B_ξ, B_ζ) and the transverse magnetic fields (B_ϕ, E_ξ, E_ζ) respectively. The two sets of fields are indirectly coupled by the dependence of the sources and the conductivity of the air on the total fields. All of the field components must therefore be solved concurrently in the finite difference code.

In the limit as the distance, r, from the weapon becomes large E_ζ and B_ζ behave as Coulomb fields (i.e., approach zero as $1/r^2$). The other field quantities are radiation fields and behave as $1/r$. Each set, (E_ϕ, B_ξ) and (E_ξ, B_ϕ) may be separated into incoming and outgoing waves. At large distances, the incoming waves must vanish. These phenomena have been observed to hold very well in the code.

To make the fields vary more slowly and thus facilitate calculation by finite difference methods, they are transformed to new variables which behave as the appropriate value, r or r^2 times the original field. Fortunately, this transformation considerably simplifies the differential equations. Perhaps some insight into the reason for this may be gained by observing

that in the TM case the transformation for the electric fields is precisely the one that transforms the static field of a charged conducting ellipsoid into a uniform field.

The magnitude of the spatial gradients in the problem is further drastically reduced by employing the retarded time of the burst point as the independent time-like variable. Indeed, with this transformation, grid spacing as large as 500 meters by 1000 meters has been used. This spacing is larger than a wavelength for some of the higher frequencies and would therefore not be feasible for a real-time code. An additional benefit resulting from the transformation to retarded time is that regridding in time near the wave front is greatly facilitated.

SECTION II. TRANSFORMATIONS OF THE FIELD EQUATIONS

1. Transverse Electric Fields

In this code the independent time-like variable, τ, will be the retarded time of the burst point defined by

$$\tau = t - \frac{r}{c} = t - \frac{\zeta - a\xi}{c} \tag{1}$$

in which r is the distance from the weapon of the field point under consideration. After making the transformations

$$\nabla \rightarrow \nabla - \frac{\hat{r}}{c}\frac{\partial}{\partial \tau} \tag{2}$$

$$\frac{\partial}{\partial t} \rightarrow \frac{\partial}{\partial \tau} \tag{3}$$

and exploiting the azimuthal symmetry of the problem, Maxwell's curl equations in prolate spheroidal coordinates become

$$\frac{\partial}{\partial \tau}(D_\xi \hat{\xi} + D_\zeta \hat{\zeta} + D_\phi \hat{\phi}) = -(j_\xi \hat{\xi} + j_\zeta \hat{\zeta} + j_\phi \hat{\phi}) + \frac{\hat{\xi}}{\sqrt{(\zeta^2 - \xi^2 a^2)(1 - \xi^2)}}\left[\frac{\partial}{\partial \zeta}\left(\sqrt{(\zeta^2 - a^2)(1 - \xi^2)}H_\phi\right)\right] - \frac{\hat{\zeta}}{\sqrt{(\zeta^2 - \xi^2 a^2)(\zeta^2 - a^2)}}\frac{\partial}{\partial \xi}\left(\sqrt{(\zeta^2 - a^2)(1 - \xi^2)}H_\phi\right)$$

$$+ \hat{\phi}\frac{\sqrt{(\zeta^2 - a^2)(1 - \xi^2)}}{\zeta^2 - \xi^2 a^2}\left[\frac{\partial}{\partial \xi}\left(\sqrt{\frac{\zeta^2 - \xi^2 a^2}{\zeta^2 - a^2}}\,H_\zeta\right) - \frac{\partial}{\partial \zeta}\left(\sqrt{\frac{\zeta^2 - \xi^2 a^2}{1 - \xi^2}}\,H_\xi\right)\right]$$

$$-\frac{1}{c}\left[\left(\alpha_{11}\frac{\partial H_\zeta}{\partial \tau} - \alpha_{21}\frac{\partial H_\xi}{\partial \tau}\right)\hat{\phi} + \alpha_{21}\frac{\partial H_\phi}{\partial \tau}\hat{\xi} - \alpha_{11}\frac{\partial H_\phi}{\partial \tau}\hat{\zeta}\right] \tag{4}$$

and

$$\frac{\partial}{\partial\tau}\left(B_\xi\hat{\xi}+B_\zeta\hat{\zeta}+B_\phi\hat{\phi}\right)=-\frac{\hat{\xi}}{\sqrt{(\zeta^2-\xi^2a^2)(1-\xi^2)}}\frac{\partial}{\partial\zeta}\left(\sqrt{(\zeta^2-a^2)(1-\xi^2)}E_\phi\right)$$

$$+\frac{\hat{\zeta}}{\sqrt{(\zeta^2-\xi^2a^2)(\zeta^2-a^2)}}\frac{\partial}{\partial\xi}\left(\sqrt{(\zeta^2-a^2)(1-\xi^2)}E_\phi\right)-\hat{\phi}\frac{\sqrt{(\zeta^2-a^2)(1-\xi^2)}}{\zeta^2-\xi^2a^2}$$

$$\left[\frac{\partial}{\partial\xi}\left(\sqrt{\frac{\zeta^2-\xi^2a^2}{\zeta^2-a^2}}E_\zeta\right)-\frac{\partial}{\partial\zeta}\left(\sqrt{\frac{\zeta^2-\xi^2a^2}{1-\xi^2}}E_\xi\right)\right]+\frac{1}{c}\left[\alpha_{21}\frac{\partial E_\phi}{\partial\tau}\hat{\xi}-\alpha_{11}\frac{\partial E_\phi}{\partial\tau}\hat{\zeta}\right.$$

$$\left.+\left(\alpha_{11}\frac{\partial E_\zeta}{\partial\tau}-\alpha_{21}\frac{\partial E_\xi}{\partial\tau}\right)\hat{\phi}\right] \tag{5}$$

in which α_{11} and α_{21} are defined by

$$\hat{r}=\alpha_{11}\hat{\xi}+\alpha_{21}\hat{\zeta} \tag{6}$$

For a description of the coordinate system and notation used see EMP Theoretical Note No. 62. Observe that Eqs. (4) and (5) separate into two sets involving E_ϕ, B_ξ, B_ζ, j_ϕ and E_ξ, E_ζ, B_ϕ, j_ξ, j_ζ. We shall refer to these as the transverse electric fields and transverse magnetic fields, respectively. The former set will be treated in this section. The differential equations governing these fields are

$$\frac{\partial}{\partial\tau}D_\phi=-j_\phi+\frac{\sqrt{(\zeta^2-a^2)(1-\xi^2)}}{\zeta^2-\xi^2a^2}\left[\frac{\partial}{\partial\xi}\left(\sqrt{\frac{\zeta^2-\xi^2a^2}{\zeta^2-a^2}}H_\zeta\right)-\frac{\partial}{\partial\zeta}\left(\sqrt{\frac{\zeta^2-\xi^2a^2}{1-\xi^2}}H_\xi\right)\right]$$

$$-\frac{1}{c}\left(\alpha_{11}\frac{\partial H_\zeta}{\partial\tau}-\alpha_{21}\frac{\partial H_\xi}{\partial\tau}\right) \tag{7}$$

$$\frac{\partial}{\partial\tau}(B_\xi\hat{\xi} + B_\zeta\hat{\zeta}) = -\frac{\hat{\xi}}{\sqrt{(\zeta^2 - \xi^2a^2)(1 - \xi^2)}}\frac{\partial}{\partial\zeta}\left(\sqrt{(\zeta^2 - a^2)(1 - \xi^2)}E_\phi\right)$$

$$+\frac{\hat{\zeta}}{\sqrt{(\zeta^2 - \xi^2a^2)(\zeta^2 - a^2)}}\frac{\partial}{\partial\xi}\left(\sqrt{(\zeta^2 - a^2)(1 - \xi^2)}E_\phi\right) + \frac{\alpha_{21}}{c}\frac{\partial E_\phi}{\partial\tau}\hat{\xi}$$

$$-\frac{\alpha_{11}}{c}\frac{\partial E_\phi}{\partial\tau}\hat{\zeta} \tag{8}$$

It has been assumed that

$$\vec{B} = \mu\vec{H} \qquad \vec{D} = \epsilon\vec{E} \tag{9}$$

also put

$$u = \frac{1}{\sqrt{\mu\epsilon}} \tag{10}$$

then

$$\frac{\partial E_\phi}{\partial\tau} = -\frac{j_\phi}{\epsilon} + \frac{u^2\sqrt{(\zeta^2 - a^2)(1 - \xi^2)}}{\zeta^2 - \xi^2a^2}\left[\frac{\partial}{\partial\xi}\left(\sqrt{\frac{\zeta^2 - \xi^2a^2}{\zeta^2 - a^2}}B_\zeta\right) - \frac{\partial}{\partial\zeta}\left(\sqrt{\frac{\zeta^2 - \xi^2a^2}{1 - \xi^2}}B_\xi\right)\right]$$

$$-\frac{u^2\alpha_{11}}{c}\frac{\partial B_\zeta}{\partial\tau} + \frac{u^2\alpha_{21}}{c}\frac{\partial B_\xi}{\partial\tau} \tag{11}$$

$$\frac{\partial B_\xi}{\partial\tau} = -\frac{1}{\sqrt{(\zeta^2 - \xi^2a^2)(1 - \xi^2)}}\frac{\partial}{\partial\zeta}\left(\sqrt{(\zeta^2 - a^2)(1 - \xi^2)}E_\phi\right) + \frac{\alpha_{21}}{c}\frac{\partial E_\phi}{\partial\tau} \tag{12}$$

$$\frac{\partial B_\zeta}{\partial\tau} = \frac{1}{\sqrt{(\zeta^2 - \xi^2a^2)(\zeta^2 - a^2)}}\frac{\partial}{\partial\xi}\left(\sqrt{(\zeta^2 - a^2)(1 - \xi^2)}E_\phi\right) - \frac{\alpha_{11}}{c}\frac{\partial E_\phi}{\partial\tau} \tag{13}$$

At this point we note that

$$\alpha_{11} = -\frac{a}{h_\xi} = -a\sqrt{\frac{1-\xi^2}{\zeta^2-\xi^2a^2}} \tag{14}$$

$$\alpha_{21} = \frac{1}{h_\zeta} = \sqrt{\frac{\zeta^2-a^2}{\zeta^2-\xi^2a^2}} \tag{15}$$

Substitute these into Eq. (11) through (13) to obtain

$$\frac{\partial E_\phi}{\partial \tau} = -\frac{j_\phi}{\epsilon} + \frac{u^2\sqrt{(\zeta^2-a^2)(1-\xi^2)}}{\zeta^2-\xi^2a^2}\frac{\partial}{\partial\xi}\left(\sqrt{\frac{\zeta^2-\xi^2a^2}{\zeta^2-a^2}}\,B_\zeta\right) - \frac{\partial}{\partial\zeta}\left(\sqrt{\frac{\zeta^2-\xi^2a^2}{1-\xi^2}}\,B_\xi\right)$$

$$+\frac{au^2}{c}\sqrt{\frac{1-\xi^2}{\zeta^2-\xi^2a^2}}\frac{\partial B_\zeta}{\partial\tau} + \frac{u^2}{c}\sqrt{\frac{\zeta^2-a^2}{\zeta^2-\xi^2a^2}}\frac{\partial B_\xi}{\partial\tau} \tag{16}$$

$$\frac{\partial B_\xi}{\partial\tau} = -\frac{1}{\sqrt{(\zeta^2-\xi^2a^2)(1-\xi^2)}}\frac{\partial}{\partial\zeta}\left(\sqrt{(\zeta^2-a^2)(1-\xi^2)}E_\phi\right) + \frac{1}{c}\sqrt{\frac{\zeta^2-a^2}{\zeta^2-\xi^2a^2}}\frac{\partial E_\phi}{\partial\tau} \tag{17}$$

$$\frac{\partial B_\zeta}{\partial\tau} = \frac{1}{\sqrt{(\zeta^2-\xi^2a^2)(\zeta^2-a^2)}}\frac{\partial}{\partial\xi}\left(\sqrt{(\zeta^2-a^2)(1-\xi^2)}E_\phi\right) + \frac{a}{c}\sqrt{\frac{1-\xi^2}{\zeta^2-\xi^2a^2}}\frac{\partial E_\phi}{\partial\tau} \tag{18}$$

In order to cast the field equations in simpler form, we make the transformation

$$\begin{pmatrix} E_\phi \\ j_\phi \end{pmatrix} = \sqrt{(\zeta^2-a^2)(1-\xi^2)}\begin{pmatrix} E'_\phi \\ j'_\phi \end{pmatrix} \tag{19}$$

$$B_\zeta = \sqrt{(\zeta^2 - \xi^2 a^2)(\zeta^2 - a^2)}B'_\zeta \qquad (20)$$

$$B_\xi = \sqrt{(\zeta^2 - \xi^2 a^2)(1 - \xi^2)}B'_\xi \qquad (21)$$

where the primed quantities are those used previously. Then Eqs. (16) through (18) become

$$\frac{\partial E_\phi}{\partial \tau} = -\frac{j_\phi}{\epsilon} + \frac{u^2(\zeta^2 - a^2)(1 - \xi^2)}{\zeta^2 - \xi^2 a^2}\left[\frac{1}{\zeta^2 - a^2}\frac{\partial B_\zeta}{\partial \xi} - \frac{1}{1 - \xi^2}\frac{\partial B_\xi}{\partial \zeta}\right] + \frac{au^2(1 - \xi^2)}{c(\zeta^2 - \xi^2 a^2)}$$

$$\frac{\partial B_\zeta}{\partial \tau} + \frac{u^2}{c}\frac{\zeta^2 - a^2}{\zeta^2 - \xi^2 a^2}\frac{\partial B_\xi}{\partial \tau} \qquad (22)$$

$$\frac{\partial B_\xi}{\partial \tau} = -\frac{\partial E_\phi}{\partial \zeta} + \frac{1}{c}\frac{\partial E_\phi}{\partial \tau} \qquad (23)$$

$$\frac{\partial B_\zeta}{\partial \tau} = \frac{\partial E_\phi}{\partial \xi} + \frac{a}{c}\frac{\partial E_\phi}{\partial \tau} \qquad (24)$$

Make the replacement

$$\vec{j} \rightarrow \vec{j}_c + \sigma\vec{E} \qquad (25)$$

The final form of Maxwell's curl equations for the transverse electric fields is

$$\frac{\partial E_\phi}{\partial \tau} = -\frac{j_\phi}{\epsilon} - \frac{\sigma}{\epsilon}E_\phi + u^2\frac{1 - \xi^2}{\zeta^2 - \xi^2 a^2}\frac{\partial B_\zeta}{\partial \xi} - u^2\frac{\zeta^2 - a^2}{\zeta^2 - \xi^2 a^2}\frac{\partial B_\xi}{\partial \zeta} + \frac{au^2}{c}\frac{1 - \xi^2}{\zeta^2 - \xi^2 a^2}\frac{\partial B_\zeta}{\partial \tau}$$

$$+ \frac{u^2}{c}\frac{\zeta^2 - a^2}{\zeta^2 - \xi^2 a^2}\frac{\partial B_\xi}{\partial \tau} \qquad (26)$$

$$\frac{\partial B_\xi}{\partial \tau} = -\frac{\partial E_\phi}{\partial \zeta} + \frac{1}{c}\frac{\partial E_\phi}{\partial \tau} \tag{27}$$

$$\frac{\partial B_\zeta}{\partial \tau} = \frac{\partial E_\phi}{\partial \xi} + \frac{a}{c}\frac{\partial E_\phi}{\partial \tau} \tag{28}$$

Define integers i, j, k such that at a mesh point

$$\xi = 1 + (1 - i)\Delta\xi\,, \qquad \zeta = a + (j - 1)\Delta\zeta\,, \qquad \tau = k\Delta\tau \tag{29}$$

With this notation, the field equations are approximated by difference equations centered at the point (i, j, k-1/2) in the following way,

$$\frac{1}{\Delta\tau}\left[E_\phi(i,\ j,\ k) - E_\phi(i,\ j,\ k-1)\right] = -\frac{1}{\epsilon}j_\phi(i,\ j,\ k-1/2) - \frac{1}{2\epsilon}\sigma(i,\ j,\ k-1/2)$$

$$\left[E_\phi(i,\ j,\ k) + E_\phi(i,\ j,\ k-1)\right] + \frac{u^2}{2\Delta\xi}\frac{1 - \xi^2}{\zeta^2 - \xi^2 a^2}\bigg|_{i,\,j}\left[B_\zeta(i-1,\ j,\ k) - B_\zeta(i,\ j,\ k)\right.$$

$$\left. + B_\zeta(i,\ j,\ k-1) - B_\zeta(i+1,\ j,\ k-1)\right] - \frac{u^2}{2\Delta\zeta}\frac{\zeta^2 - a^2}{\zeta^2 - \xi^2 a^2}\bigg|_{i,\,j}\left[B_\xi(i,\ j+1,\ k-1)\right.$$

$$\left. -B_\xi(i,\ j,\ k-1) + B_\xi(i,\ j,\ k) - B_\xi(i,\ j-1,\ k)\right] + \frac{au^2}{c\Delta\tau}\frac{1 - \xi^2}{\zeta^2 - \xi^2 a^2}\bigg|_{i,\,j}\left[B_\zeta(i,\ j,\ k)\right.$$

$$\left. -B_\zeta(i,\ j,\ k-1)\right] + \frac{u^2}{c\Delta\tau}\frac{\zeta^2 - a^2}{\zeta^2 - \xi^2 a^2}\bigg|_{i,\,j}\left[B_\xi(i,\ j,\ k) - B_\xi(i,\ j,\ k-1)\right] \tag{30}$$

$$\frac{1}{\Delta\tau}\left[B_\xi(i,\ j,\ k) - B_\xi(i,\ j,\ \kappa-1)\right] = -\frac{1}{2\Delta\zeta}\left[E_\phi(i,\ j+1,\ \kappa-1) - E_\phi(i,\ j,\ k-1)\right.$$

$$\left. + E_\phi(i,\ j,\ k) - E_\phi(i,\ j-1,\ k)\right] + \frac{1}{c\Delta\tau}\left[E_\phi(i,\ j,\ k) - E_\phi(i,\ j,\ k-1)\right] \qquad (31)$$

$$\frac{1}{\Delta\tau}\left[B_\xi(i,\ j,\ k) - B_\xi(i,\ j,\ k-1)\right] = \frac{1}{2\Delta\xi}\left[E_\phi(i-1,\ j,\ k) - E_\phi(i,\ j,\ k)\right.$$

$$\left. + E_\phi(i,\ j,\ k-1) - E_\phi(i+1,\ j,\ k-1)\right] + \frac{a}{c\Delta\tau}\left[E_\phi(i,\ j,\ k) - E_\phi(i,\ j,\ k-1)\right] \qquad (32)$$

provided the fields are known at (i, j-1, k), (i-1, j, k), and at all mesh points for the preceding time step. Equations (30), (31), and (32) may be solved simultaneously for the three field components at the point (i, j, k). Thus, from a knowledge of the fields on the boundaries and at the initial time, one can apply these equations successively to obtain the fields throughout the mesh at later times.

2. Transverse Magnetic Fields

The field components (E_ξ, E_ζ, B_ϕ) in this portion of the code satisfy the same differential equations as those calculated in the air by the prolate spheroidal code for a low-altitude burst. The latter code is discussed in an EMP theoretical note (Knight, 1969). The results of that calculation will be quoted here for completeness.

The derivation begins by writing Maxwell's curl equations in prolate spheroidal coordinates in the retarded time of the burst point and taking advantage of the azimuthal symmetry. The resulting differential equations are then subjected to the transformation

$$\begin{pmatrix} E_\xi \\ j_\xi \end{pmatrix} = \sqrt{(\zeta^2 - \xi^2 a^2)(1 - \xi^2)} \begin{pmatrix} E'_\xi \\ j'_\xi \end{pmatrix} \tag{33}$$

$$\begin{pmatrix} E_\zeta \\ j_\zeta \end{pmatrix} = \sqrt{(\zeta^2 - \xi^2 a^2)(\zeta^2 - a^2)} \begin{pmatrix} E'_\zeta \\ j'_\zeta \end{pmatrix} \tag{34}$$

$$B_\phi = \sqrt{(\zeta^2 - a^2)(1 - \xi^2)}\, B'_\phi \tag{35}$$

in which the primed quantities are the original ones. The final form of Maxwell's equations for these field components is then

$$\frac{\partial E_\xi}{\partial \tau} = -\frac{\sigma}{\epsilon} E_\xi - \frac{j_\xi}{\epsilon} + u^2 \frac{\partial B_\phi}{\partial \zeta} - \frac{u^2}{c} \frac{\partial B_\phi}{\partial \tau} \tag{36}$$

$$\frac{\partial E_\zeta}{\partial \tau} = -\frac{\sigma}{\epsilon} E_\zeta - \frac{j_\zeta}{\epsilon} - u^2 \frac{\partial B_\phi}{\partial \xi} - \frac{au^2}{c} \frac{\partial B_\phi}{\partial \tau} \tag{37}$$

$$\frac{\partial B_\phi}{\partial \tau} = \frac{\zeta^2 - a^2}{\zeta^2 - \xi^2 a^2} \frac{\partial E_\xi}{\partial \zeta} - \frac{1 - \xi^2}{\zeta^2 - \xi^2 a^2} \frac{\partial E_\zeta}{\partial \xi} - \frac{a}{c} \frac{1 - \xi^2}{\zeta^2 - \xi^2 a^2} \frac{\partial E_\zeta}{\partial \tau} - \frac{1}{c} \frac{\zeta^2 - a^2}{\zeta^2 - \xi^2 a^2} \frac{\partial E_\xi}{\partial \tau} \tag{38}$$

By using the notation of Eq. (29), Eqs. (36) through (38) can be replaced by difference equations centered at (i, j, k-1/2). Thus,

$$\frac{1}{\Delta\tau}\left[E_\xi(i,\ j,\ k) - E_\xi(i,\ j,\ k-1)\right] = -\frac{\sigma(i,\ j,\ k-1/2)}{2\epsilon}\left[E_\xi(i,\ j,\ k) + E_\xi(i,\ j,\ k-1)\right]$$

$$- \frac{j_\xi(i,\ j,\ k-1/2)}{\epsilon} + \frac{u^2}{2\Delta\zeta}\left[B_\phi(i,\ j+1,\ k-1) - B_\phi(i,\ j,\ k-1) + B_\phi(i,\ j,\ k)\right.$$

$$\left. - B_\phi(i,\ j-1,\ k)\right] - \frac{u^2}{c\Delta\tau}\left[B_\phi(i,\ j,\ k) - B_\phi(i,\ j,\ k-1)\right] \qquad (39)$$

$$\frac{1}{\Delta\tau}\left[E_\zeta(i,\ j,\ k) - E_\zeta(i,\ j,\ k-1)\right] = -\frac{\sigma(i,\ j,\ k-1/2)}{2\epsilon}\left[E_\zeta(i,\ j,\ k) + E_\zeta(i,\ j,\ k-1)\right]$$

$$- \frac{j_\zeta(i,\ j,\ k-1/2)}{\epsilon} - \frac{u^2}{2\Delta\xi}\left[B_\phi(i-1,\ j,\ k) - B_\phi(i,\ j,\ k) + B_\phi(i,\ j,\ k-1)\right.$$

$$\left. - B_\phi(i+1,\ j,\ k-1)\right] - \frac{au^2}{c\Delta\tau}\left[B_\phi(i,\ j,\ k) - B_\phi(i,\ j,\ k-1)\right] \qquad (40)$$

$$\frac{1}{\Delta\tau}\left[B_\phi(i,\ j,\ k) - B_\phi(i,\ j,\ k-1)\right] = \frac{1}{2\Delta\zeta}\left(\frac{\zeta^2 - a^2}{\zeta^2 - \xi^2 a^2}\right)\Bigg|_{i,\,j}\left[E_\xi(i,\ j+1,\ k-1)\right.$$

$$\left. -E_\xi(i,\ j,\ k-1) + E_\xi(i,\ j,\ k) - E_\xi(i,\ j-1,\ k)\right] + \frac{1}{2\Delta\xi}\left(\frac{1 - \xi^2}{\zeta^2 - \xi^2 a^2}\right)\Bigg|_{i,\,j}$$

$$\left[E_\zeta(i+1,\ j,\ k-1) - E_\zeta(i,\ j,\ k-1) + E_\zeta(i,\ j,\ k) - E_\zeta(i-1,\ j,\ k)\right]$$

$$- \frac{a}{c\Delta\tau}\left(\frac{1 - \xi^2}{\zeta^2 - \xi^2 a^2}\right)\Bigg|_{i,\,j}\left[E_\zeta(i,\ j,\ k) - E_\zeta(i,\ j,\ k-1)\right] - \frac{1}{c\Delta\tau}\left(\frac{\zeta^2 - a^2}{\zeta^2 - \xi^2 a^2}\right)\Bigg|_{i,\,j}$$

$$\left[E_\xi(i,\ j,\ k) - E_\xi(i,\ j,\ k-1)\right] \qquad (41)$$

SECTION III: BOUNDARY CONDITIONS

The azimuthal symmetry of the problem implies that at the z-axis the normal field components as well as E_ϕ and B_ϕ vanish, i.e.:

$$\left.\begin{aligned} E_\xi &\to 0 \\ E_\phi &\to 0 \\ B_\xi &\to 0 \\ B_\phi &\to 0 \end{aligned}\right\} \quad \text{as } \xi \to 1 \text{ for } \zeta > a \tag{43}$$

$$\left.\begin{aligned} E_\zeta &\to 0 \\ E_\phi &\to 0 \\ B_\zeta &\to 0 \\ B_\phi &\to 0 \end{aligned}\right\} \quad \text{as } \zeta \to a \text{ for } -1 \le \xi \le 1 \tag{44}$$

The remaining field components have been calculated on the z-axis by the code in various ways. Perhaps the simplest of these (and incidentally, the first one used in the code) evaluates the equations

$$\frac{1}{\Delta\tau}\left[B_\zeta(1,\ j,\ k) - B_\zeta(1,\ j,\ k-1)\right] = \frac{-1}{2\Delta\xi}\left[E_\phi(2,\ j,\ k) + E_\phi(2,\ j,\ k-1)\right] \tag{45}$$

$$\frac{1}{\Delta\tau}\left[B_\xi(i,\ 1,\ k) - B_\xi(i,\ 1,\ k-1)\right] = -\frac{1}{2\Delta\zeta}\left[E_\phi(i,\ 2,\ k) + E_\phi(i,\ 2,\ k-1)\right] \tag{46}$$

$$\frac{1}{\Delta\tau}\left[E_\zeta(1,\ j,\ k) - E_\zeta(1,\ j,\ k-1)\right] = -\frac{1}{2\epsilon}\sigma(1,\ j,\ k-1/2)\left[E_\zeta(1,\ j,\ k) + E_\zeta(1,\ j,\ k-1)\right] - \frac{1}{\epsilon}j_\zeta(1,\ j,\ k-1/2) - \frac{u^2}{\Delta\xi}B_\phi(2,\ j,\ k-1) \tag{47}$$

$$\frac{1}{\Delta\tau}\left[E_\xi(\quad,\quad,\quad) - E_\xi(\quad,\quad,\quad)\right] = -\frac{1}{2\epsilon}\left[\quad\right]$$

$$+ E_\xi(i,\ 1,\ k-1)\Big] - \frac{1}{\epsilon} j_\xi(i,\ 1,\ k-1/2) + \frac{u^2}{\Delta\xi} B_\phi(i,\ 2,\ k-1) \qquad (48)$$

on the z-axis. The appropriate field equations are then applied at the adjacent mesh point. In each of the four cases, the method yields four simultaneous algebraic equations which determine the unknown field at the z-axis as well as the corresponding three field components at the adjoining mesh point.

Following is a derivation of the boundary conditions presently used in the code for the tangential field components at the z-axis. The first one considered is E_ζ at $\xi = 1$, $\zeta > a$ (i.e., the radial electric field on the z-axis above the burst point). From Eq. (37) it is evident that to determine E_ζ on the z-axis, one must evaluate $\partial B_\phi / \partial \xi$ in the limit $\xi \to 1$. Let η be a coordinate that is antiparallel to ξ with the dimension of length. For a differentiable function, $f(\xi, \zeta, \phi, \tau)$ it follows that

$$\frac{\partial f}{\partial \eta} = -\nabla f \cdot \hat{\xi} = -\frac{1}{h_\xi}\frac{\partial f}{\partial \xi} \qquad (49)$$

or, putting $f = B_\phi$

$$\lim_{\xi \to 1} \frac{\partial B_\phi}{\partial \xi} = -\lim_{\eta \to 0} h_\xi \frac{\partial B_\phi}{\partial \eta} \qquad (50)$$

The scale factor, h_ξ, is given by

$$h_\xi = \sqrt{\frac{\zeta^2 - \xi^2 a^2}{1 - \xi^2}} \qquad (51)$$

The right-hand side of Eq. (50) can be evaluated with the help of Ampere's law which in retarded time is

$$\oint_c \vec{H}' \cdot d\vec{\ell} = \int_s \vec{j}' \cdot d\vec{s} + \frac{\partial}{\partial \tau} \int_s \vec{D}' \cdot d\vec{s} + \frac{1}{c} \frac{\partial}{\partial \tau} \int_s \hat{r} \cdot H' \, d\vec{s} \qquad (52)$$

Throughout this section primed functions represent the real quantities and those transformed by Equations (19) through (21) or (33) through (35) are unprimed.

Evaluate Eq. (52) at the small circle, c, of radius η shown below.

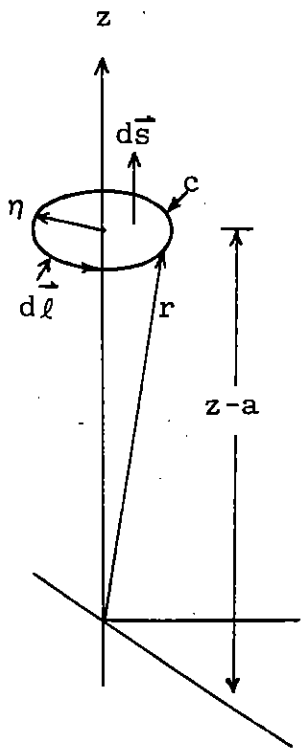

Also assume that j'_ζ and E'_ζ are approximately uniform within the circle. The azimuthal symmetry of the problem requires that B_ϕ is constant on c. Equation (52) reduces to

$$2\pi\eta B'_\phi(\eta, z, \tau) = \mu\pi\eta^2 j'_\zeta(\eta, z, \tau) + \mu\epsilon\pi\eta^2 \frac{\partial}{\partial\tau} E'_\zeta(\eta, z, \tau) \tag{53}$$

The last term in Eq. (52) yields a quantity of higher order in η and may be neglected. Write Eq. (53) as

$$B'_\phi(\eta, z, \tau) = \frac{\mu\eta}{2} j'_\zeta(\eta, z, \tau) + \frac{\mu\epsilon\eta}{2} \frac{\partial}{\partial\tau} E'_\zeta(\eta, z, \tau) \tag{54}$$

Since B'_ϕ vanishes as $\eta \to 0$, we have

$$\lim_{\eta \to 0} \frac{\partial B'_\phi(\eta, z, \tau)}{\partial\eta} = \lim_{\eta \to 0} \frac{B'_\phi(\eta, z, \tau)}{\eta} \tag{55}$$

Using Eq. (54) this becomes

$$\lim_{\eta \to 0} \frac{\partial B'_\phi}{\partial\eta} = \lim_{\eta \to 0} \left(\frac{\mu}{2} j'_\zeta(\eta, z, \tau) + \frac{\mu\epsilon}{2} \frac{\partial}{\partial\tau} E'_\zeta(\eta, z, \tau) \right) \tag{56}$$

Combining Eqs. (50), (51) and (56) yields:

$$\lim_{\xi \to 1} \frac{\partial B'_\phi(\xi, \zeta, \tau)}{\partial\xi} = \lim_{\xi \to 1} - \sqrt{\frac{\zeta^2 - \xi^2 a^2}{1 - \xi^2}} \left[\frac{\mu}{2} j'_\zeta(\xi, \zeta, \tau) + \frac{\mu\epsilon}{2} \frac{\partial}{\partial\tau} E'_\zeta(\xi, \zeta, \tau) \right] \tag{57}$$

The transformed fields are related to the real fields according to Eqs. (34) and (35). Using these, Eq. (57) can be written in terms of the transformed fields. Thus

$$\lim_{\xi \to 1} \frac{\partial}{\partial \xi}\left[\frac{B_\phi}{\sqrt{(\zeta^2 - a^2)(1 - \xi^2)}}\right] = \lim_{\xi \to 1}\left\{-\sqrt{\frac{\zeta^2 - \xi^2 a^2}{1 - \xi^2}} \cdot \frac{1}{\sqrt{(\zeta^2 - \xi^2 a^2)(\zeta^2 - a^2)}}\left[\frac{\mu j_\zeta}{2} + \frac{\mu\epsilon}{2}\frac{\partial E_\zeta}{\partial \tau}\right]\right\} \tag{58}$$

or

$$\lim_{\xi \to 1}\left[\frac{\partial B_\phi}{\partial \xi} + \frac{\xi B_\phi}{1 - \xi^2}\right] = \lim_{\xi \to 1} -\frac{1}{2}\left(\mu j_\zeta + \mu\epsilon\frac{\partial E_\zeta}{\partial \tau}\right) \tag{59}$$

Using L'Hospital's rule, one finds that the limit of the second term in Eq. (59) is just minus twice the limit of the first term. Hence, we have

$$\lim_{\xi \to 1} u^2 \frac{\partial B_\phi}{\partial \xi} = \lim_{\xi \to 1} \frac{1}{2}\left(\frac{j_\zeta}{\epsilon} + \frac{\partial E_\zeta}{\partial \tau}\right) \tag{60}$$

According to Maxwell's field equations for the transformed fields in retarded time,

$$\lim_{\xi \to 1} u^2 \frac{\partial B_\phi}{\partial \xi} = \lim_{\xi \to 1}\left(-\frac{j_\zeta}{\epsilon} - \frac{\partial E_\zeta}{\partial \tau}\right) \tag{61}$$

Comparing Eqs. (60) and (61) [illegible] the transition at

$$\lim_{\xi \to 1} \frac{\partial B_\phi}{\partial \xi} = 0 \tag{62}$$

Substituting this into Eq. (37) indicates that the equation to be solved on the z-axis at $\xi = 1$, is

$$\frac{\partial E_\zeta}{\partial \tau} = -\frac{j_\zeta}{\epsilon} - \frac{\sigma E_\zeta}{\epsilon} \tag{63}$$

This is the required boundary condition for E_ζ at $\xi = 1$, $\zeta > a$.

Next, we consider E_ξ at $\zeta = a$, i.e., the tangential electric field on the z axis below the burst. At $\zeta \to a$, Eq. (36) becomes

$$\frac{\partial E_\xi}{\partial \tau} = -\frac{\sigma}{\epsilon} E_\xi - \frac{j_\xi}{\epsilon} + u^2 \frac{\partial B_\phi}{\partial \zeta} \tag{64}$$

We wish to determine the behavior of $\partial B_\phi / \partial \zeta$ as $\zeta \to a$. Choose a coordinate, λ, parallel with ζ with a dimension of length, then an equation analogous to Eq. (49) is

$$\frac{\partial f}{\partial \lambda} = \nabla f \cdot \hat{\zeta} = \frac{1}{h_\zeta} \frac{\partial f}{\partial \zeta} \tag{65}$$

where

$$h_\zeta = \sqrt{\frac{\zeta^2 - \xi^2 a^2}{\zeta^2 - a^2}} \tag{66}$$

Evaluate Eq. (52) on a small circle, c, of radius λ whose center is at

$\zeta = a$. Assume that $\lambda \ll r \simeq z$ and that λ is small enough that E_ξ and j_ξ are constant in c. Then

$$B'_\phi(\lambda, z, \tau) = \frac{\mu\lambda}{2} j'_\xi(\lambda, z, \tau) + \frac{\mu\epsilon\lambda}{2} \frac{\partial}{\partial\tau} E'_\xi(\lambda, z, \tau) \tag{67}$$

Since B'_ϕ vanishes at $\lambda \to 0$, we have

$$\lim_{\lambda \to 0} \frac{\partial B'_\phi(\lambda, z, \tau)}{\partial \lambda} = \lim_{\lambda \to 0} \frac{B'_\phi(\lambda, z, \tau)}{\lambda} \tag{68}$$

from Eq. (67) this is seen to be

$$\lim_{\lambda \to 0} \frac{\partial B'_\phi(\lambda, z, \tau)}{\partial \lambda} = \lim_{\lambda \to 0} \left[\frac{\mu}{2} j'_\xi(\lambda, z, \tau) + \frac{\mu\epsilon}{2} \frac{\partial}{\partial\tau} E'_\xi(\lambda, z, \tau) \right] \tag{69}$$

Combining Eqs. (65), (66), and (69) yields

$$\lim_{\zeta \to a} \frac{\partial B'_\phi(\lambda, z, \tau)}{\partial \zeta} = \lim_{\zeta \to a} \sqrt{\frac{\zeta^2 - \xi^2 a^2}{\zeta^2 - a^2}} \left[\frac{\mu}{2} j'_\xi(\xi, \zeta, \tau) + \frac{\mu\epsilon}{2} \frac{\partial}{\partial\tau} E'_\xi(\xi, \zeta, \tau) \right] \tag{70}$$

The transformed fields are related to the real fields according to Eqs. (33) and (35). Write Eq. (70) for the transformed fields

$$\lim_{\zeta \to a} \frac{\partial}{\partial \zeta} \left[\frac{B_\phi}{\sqrt{(\zeta^2 - a^2)(1 - \xi^2)}} \right] = \lim_{\zeta \to a} \sqrt{\frac{\zeta^2 - \xi^2 a^2}{\zeta^2 - a^2}} \frac{\left[\frac{\mu}{2} j_\xi(\xi, \zeta, \tau) + \frac{\mu\epsilon}{2} \frac{\partial}{\partial\tau} E_\xi(\xi, \zeta, \tau) \right]}{\sqrt{(\zeta^2 - \xi^2 a^2)(1 - \xi^2)}} \tag{71}$$

$$\lim_{\zeta \to a} \frac{\partial B_\phi}{\partial \zeta} = \lim_{\zeta \to a} -\left[\mu j_\xi(\xi, \zeta, \tau) + \mu\epsilon \frac{\partial}{\partial \tau} E_\xi(\xi, \zeta, \tau)\right] \tag{72}$$

Comparing Eq. (36) and Eq. (72) yields

$$\lim_{\zeta \to a} \frac{\partial B_\phi}{\partial \zeta} = 0 \tag{73}$$

Thus at $\zeta = a$, the differential equation to be solved is

$$\frac{\partial E_\xi}{\partial \tau} = -\frac{\sigma}{\epsilon} E_\xi - \frac{j_\xi}{\epsilon} \tag{74}$$

The B_ξ and B_ζ components may be treated similarly. Presently, the fields at the maximum value of ζ are being obtained numerically by extrapolation of adjacent fields.

SECTION V. COMPARISON OF HAPS WITH OTHER EMP CODES

An excellent method of obtaining confidence in theoretical and computational models for simulating EMP is through comparisons of results. These comparisons can be accomplished with existing empirical data or with other computer codes of high confidence. It is through the code-code comparison that the accuracy of the HAPS field code will be illustrated.

The first code-code comparisons were designed to check the effectiveness of HAPS in treating spatial gradients of the sources. These are caused primarily by the variation of the air density and of the angle between the direction of motion of individual electrons and the earth's magnetic field. The B code was chosen for the first comparison since it calculates the air asymmetry signal for burst altitudes between 2.5 km and 20 km. As in the HAPS code, the B code is able to employ azimuthal symmetry due to the assumed uniformity of the weapon outputs. The use of azimuthal symmetry in HAPS also requires the assumed verticality of the earth's magnetic field. For this initial comparison the Phi current components (and therefore the effect of the earth's magnetic field) were not considered. Identical analytic sources of radial currents were input into the two codes for a 10-km burst and time histories of electric fields were compared at points of interest.

Figure 1 illustrates an overlay of HAPS and B results at a coaltitude observer outside of the source region. The only radiated electric field for this burst height, E_θ, is compared (in normalized form) with excellent

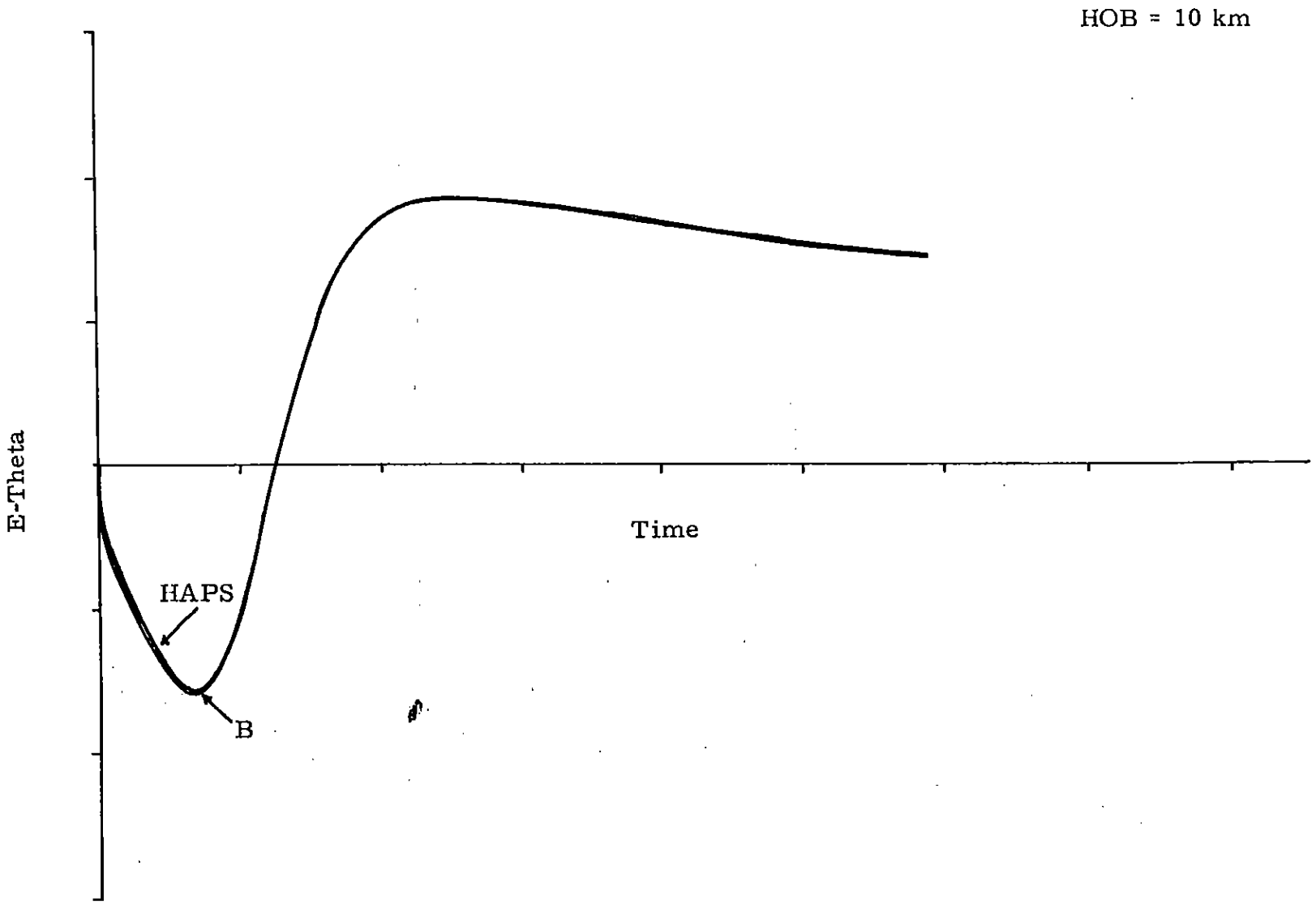

Figure 1. Normalized Comparison of the Results of the HAPS and B Codes

results. Because this code has been effective in code-data comparisons in the past, it can be determined from this comparison that HAPS is correctly treating the air density spatial gradient. It should be pointed out that the resultant time waveforms at 60 observers compared with this same accuracy illustrated.

While considering the 10-km height of burst region a comparison of results was accomplished between HEMP and HAPS. HEMP is a line-of-sight, high frequency approximation code which is generally used for bursts above 30 km. It was felt, however, that if the magnetic turning signal alone were examined, a useful comparison could be made at 10 km. To remove the spatial gradient caused by the differences in air density, EMP sources were calculated for both codes using a constant air density throughout the source region. A vertical magnetic field was then prescribed in HEMP to conform with HAPS. An overlay of the results is illustrated in Figure 2 for a position 7 km below the burst, at a 45° angle from the vertical. The E_ϕ component, which is the largest of the transverse E-fields caused by the earth's magnetic field, compares adequately. Some positions did exhibit waveform differences on the order of 5%, but these differences were attributed to observer interpolation in the HAPS code and the small spatial gradients in HAPS caused by the different angles between the original electron trajectories and the local earth's magnetic field vector.

The last waveform of interest calculated at a 10-km height of burst was a normal run of the HAPS code illustrating the magnetic turning signal

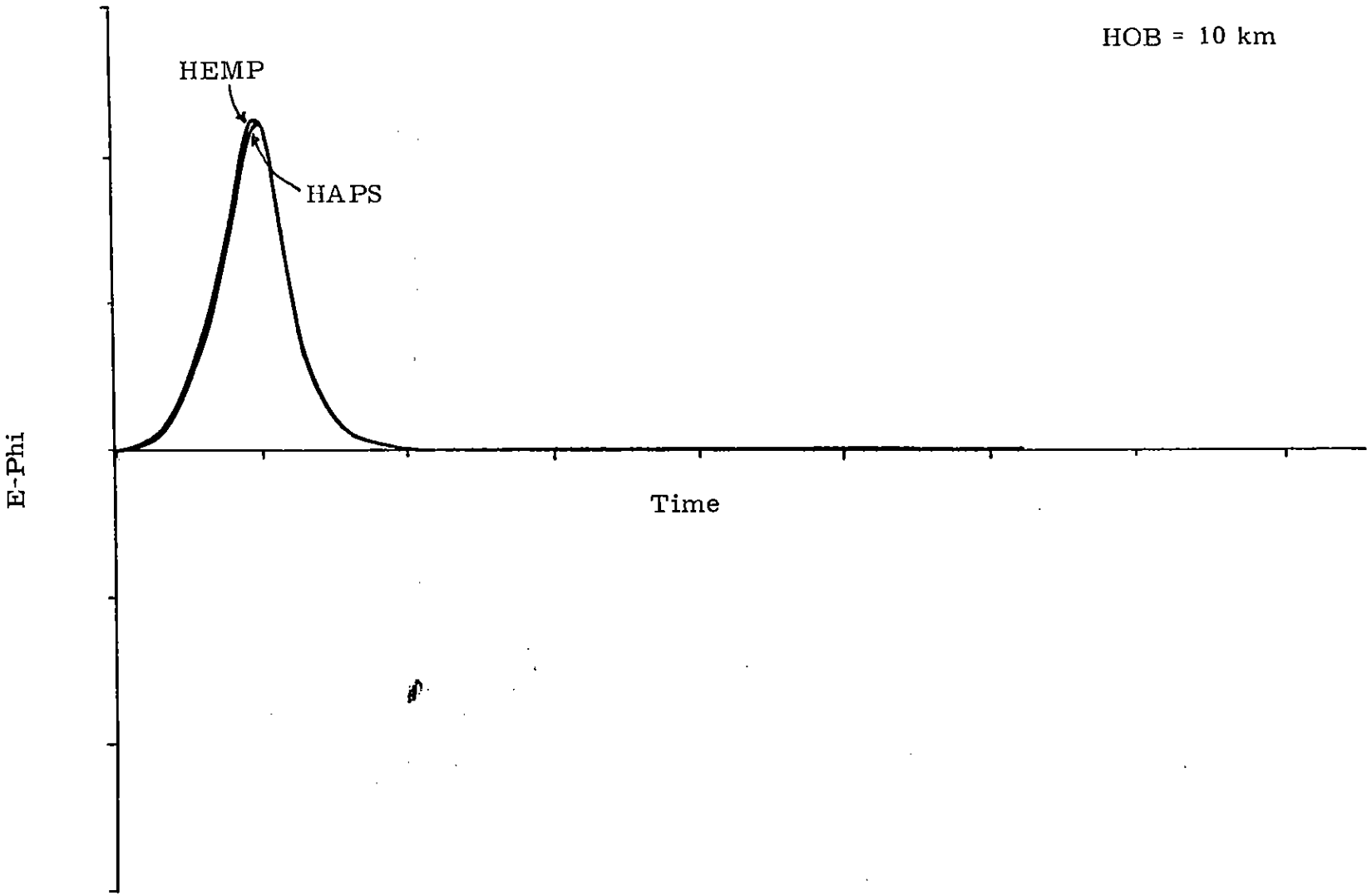

Figure 2. Normalized Comparison of the Results of the HAPS and HEMP Codes

and the air asymmetry signal for a mid-altitude observer. One may note in Figure 3 that the magnetic turning signal is very small, as the E_θ turning signal component is much smaller than the E_ϕ component, but the E_ϕ component does not exhibit any air asymmetry signal due to the assumed azimuthal symmetry. Also this observer is outside of the source region where the air asymmetry signal will predominate over the magnetic turning signal.

After completion of these comparisons, it was evident that HAPS could adequately solve the field equations given accurate and stable sources. The next step was to compare HAPS with HEMP for a high altitude burst, allowing the HAPS code to calculate both the magnetic turning signal and the air asymmetry signal. It was anticipated that some difference would be exhibited between the codes at later times of calculation, illustrating the accuracy limit of the high-frequency approximation in HEMP. For a 50-km height of burst Figure 4 illustrates a spatial contour from the HAPS code which consists of iso-contours of peak electric field. The line of sight of the HEMP code used for comparative purposes is overlayed on the HAPS contour plot, and one observer position is marked for time waveform comparison.

Figure 5 illustrates a normalized time comparison of the E_ϕ components at observer 1 as shown in Figure 4. There is a slight difference in the peak values illustrated which is a function of the interpolation of information to an exact observer position in the HAPS code. The reader

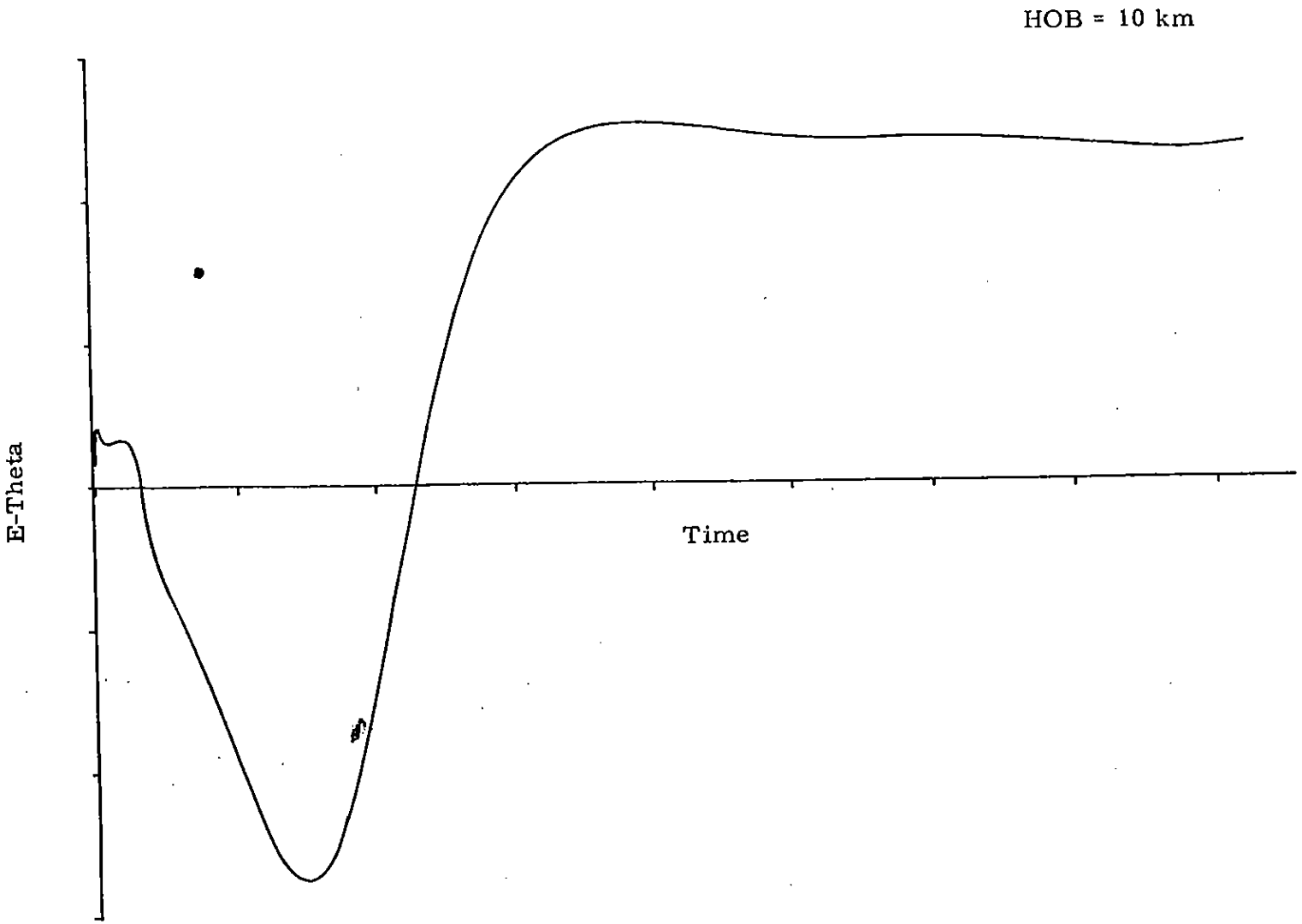

Figure 3. A Normalized Typical Waveform from the HAPS Code

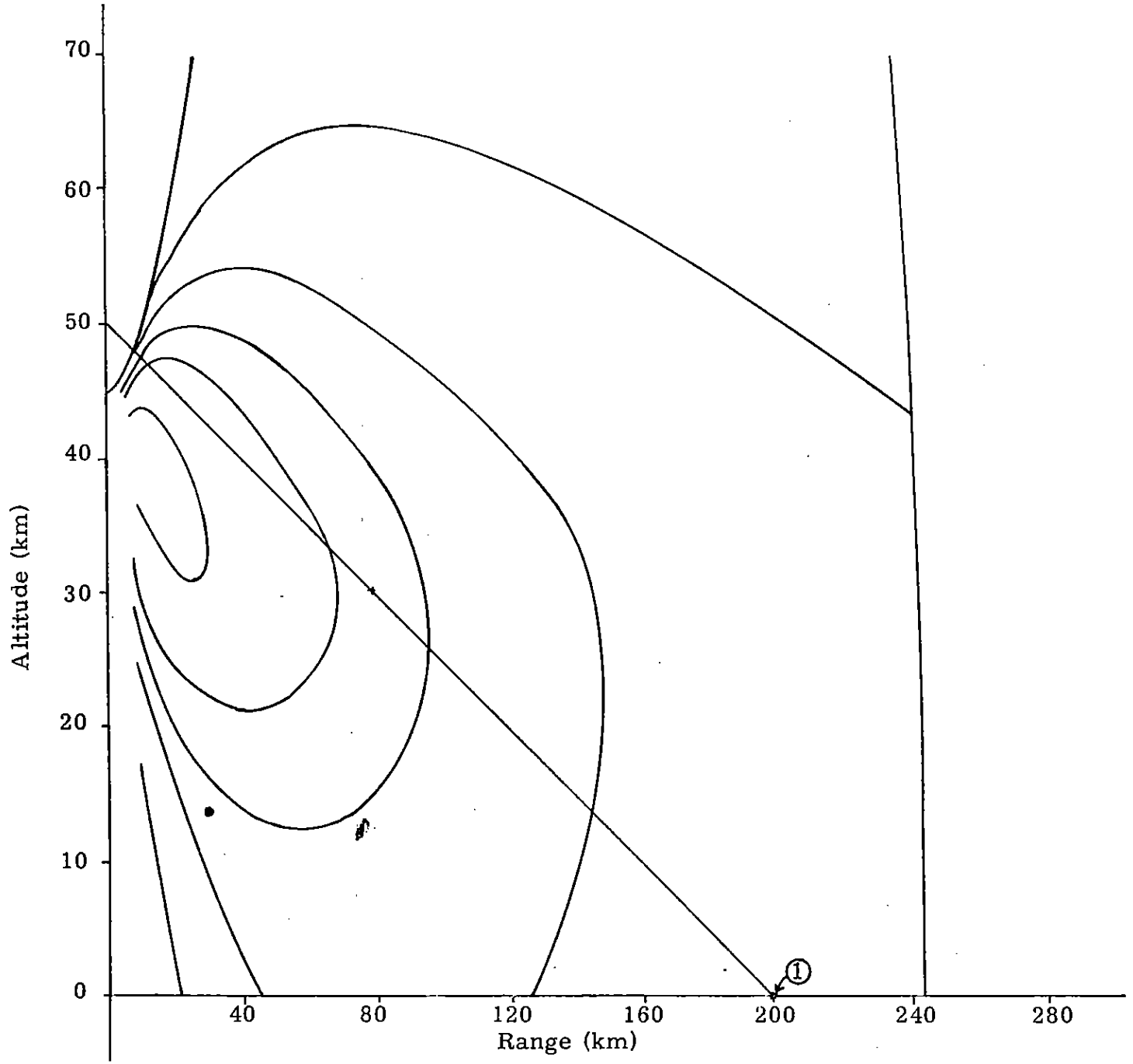

Figure 4. A Contour Plot of Peak Electric Fields from the HAPS Code Overlayed with a HEMP Line of Sight

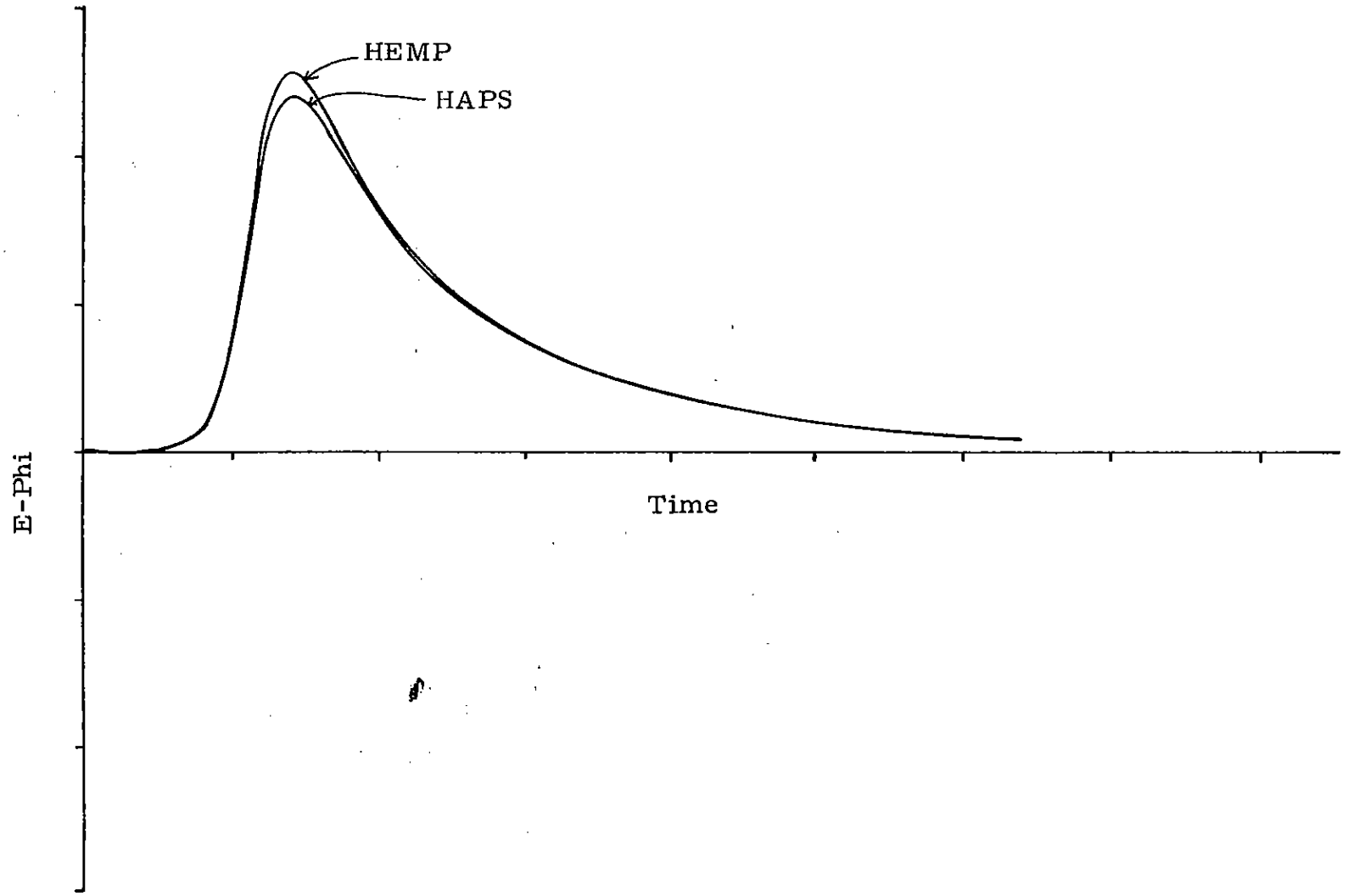

Figure 5. A Normalized Comparison of HAPS and HEMP at Observer 1

should note the exactness of the field values at the end of the pulse. It appears, as one would expect, that each code is calculating the same magnetic turning signal. Figure 6 illustrates a comparison of the theta component of electric field which in the HAPS code contains the air asymmetry signal. The difference seen in the figure is small and presumably this is due to the fact that the theta magnetic turning signal is still dominating over the air asymmetry contributions. From these comparisons we can see that much later times of calculation are required to illustrate some difference between the codes.

Work is being accomplished to calculate late-time sources in order to produce an accurate late-time field calculation and comparison between HEMP and HAPS. The result of this comparison will provide insight into the necessity of continuing the 2-D effort, and of developing a 3-D code to solve the late-time, low frequency EMP problem. Research will continue with the 2-D code and a more detailed classified report will be published indicating the magnitudes of the EMP fields calculated and their low frequency content.

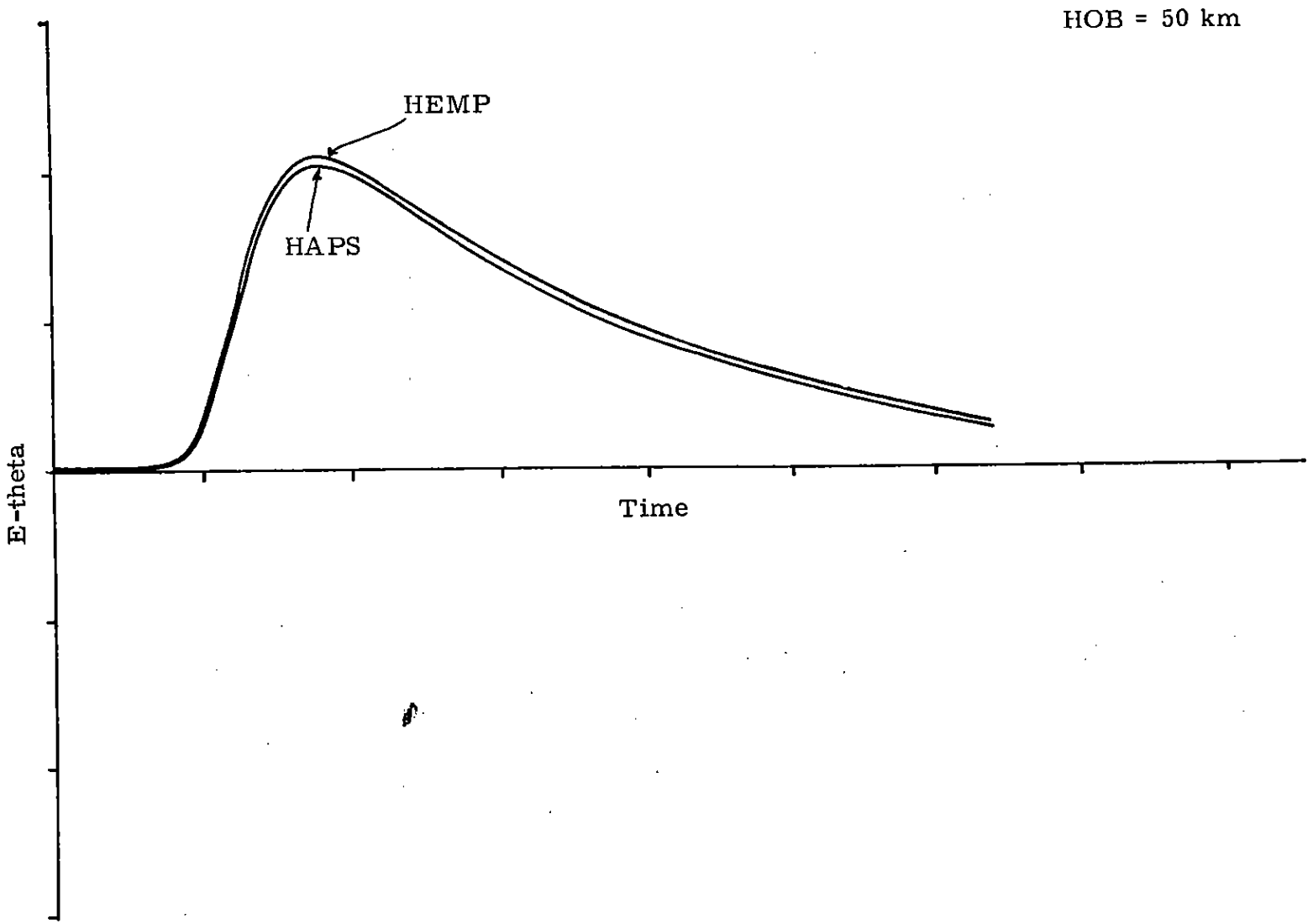

Figure 6. A Normalized Comparison of HAPS and HEMP at Observer 1

J. H. Erkkila (1967). "Calculation of the EMP from High Altitude Nuclear Detonations," Note No. 26, Electromagnetic Pulse Theoretical Notes.

W. J. Karzas and R. Latter (1964). "Detection of the Electromagnetic Radiation from Nuclear Explosions in Space," Note No. 40, Electromagnetic Pulse Theoretical Notes.

R. Knight (1969). "Numerical Solutions of Maxwell's Equations with Azimuthal Symmetry in Prolate Spheroidal Coordinates," Note No. 62, Electromagnetic Pulse Theoretical Notes.